

Trimeric Clusters of Silver in Aqueous AgNO_3 Solutions and Their Role as Nuclei in Forming Triangular Nanoplates of Silver**

Yujie Xiong, Isao Washio, Jingyi Chen, Martin Sadilek, and Younan Xia*

The extensive use of silver nanostructures as optical labels, substrates for surface-enhanced Raman scattering (SERS), near-field optical probes, and contrast agents for biomedical imaging has led to a steadily growing interest in the chemical synthesis of such species.^[1] More importantly, the optical properties of silver nanostructures can be tailored with great versatility by controlling their shapes during synthesis.^[2] A remarkable example is that of triangular nanoplates of silver, a class of nanostructures with two-dimensional anisotropy.^[3–6] The nanoplates exhibit fascinating optical properties, such as intense quadrupole resonance peaks that are absent in small nanospheres^[3] and have found use in chemical and biological sensing.^[4] Since the first publication on this subject by Mirkin and co-workers in 2001, a number of different synthetic routes have been demonstrated, including those based on photo- or thermally induced transformation and on direct chemical reduction.^[5,6] All of these methods rely on the slow generation of neutral silver atoms to enable kinetic control. Although kinetic control has also been used in the synthesis of platelike nanostructures from other noble metals, it remains largely unresolved how this process works.^[7,8] It has been proposed that light of proper wavelengths or that certain capping ligands, such as citrate, are responsible for the formation of silver nanoplates.^[5a,6c] However, our most recent work demonstrated that the platelike morphology could also be obtained in the absence of both light and citrate.^[8] Herein, we elucidate the mechanism of nanoplate formation by focusing on the silver clusters that dominate nucleation.

Despite the technological importance of nanocrystals and the extensive efforts that have been devoted to studying them, attempts to synthetically and systematically control their shapes and properties have met with limited success. One barrier to success is the fact that very little is known about the details of nucleation involved in the formation of nanocrystals.^[9] In the case of a metal, it is still unclear how a

precursor salt is reduced into neutral atoms that then aggregate and evolve into nanoscale crystals. The γ -radiation-based synthesis developed by Henglein has shed some light on the nucleation process by controlling the generation of zero-valent atoms and thus their agglomeration into small clusters.^[10] Both UV/Vis spectroscopic and scanning tunneling microscopic studies of these clusters suggested that Ag_4^{2+} and Ag_8^{4+} were the most abundant species involved in the nucleation stage.^[11] Growth of these clusters into nanocrystals likely occurred through a combination of aggregation and atomic addition. Herein we demonstrate, for the first time, that there exists a smaller cluster, Ag_3^+ or Ag_3 , in the nucleation stage of a solution-phase synthesis that employs AgNO_3 as a precursor to silver. These trimeric clusters can serve as nuclei for the addition of newly formed silver atoms and eventually lead to the formation of triangular nanoplates.

Mass spectrometry provides a tool for simple identification and characterization of silver clusters possibly contained in aqueous AgNO_3 solution. Since a mass spectrometer can separate and detect ions of different masses, it allows the different isotopes of a given element to be easily distinguished. It is also feasible to quickly identify clusters of different sizes by analyzing the isotope patterns. Natural silver comprises a nearly 1:1 mixture of two isotopes with atomic masses of 106.9 and 108.9 amu. A trimeric cluster of silver contains three silver atoms that may come in four different combinations: three ^{107}Ag atoms, two ^{107}Ag atoms plus one ^{109}Ag atom, one ^{107}Ag atom plus two ^{109}Ag atoms, or three ^{109}Ag atoms. As a result, Ag^+ ions are expected to appear in the mass spectrum as a doublet (with two peaks located at m/z 106.9 and 108.9), while Ag_3^+ clusters give rise to a quadruplet (with four peaks located at m/z 320.7, 322.7, 324.7, and 326.7 with a ratio of 1:3:3:1).

Figure 1a shows a positive-mode mass spectrum taken from an aqueous solution of AgNO_3 immediately after its preparation. In the m/z range from 80 to 1100, there are four sets of peaks with distinct isotope patterns. According to the isotope patterns and their corresponding m/z ratios, the peaks can be assigned to Ag^+ , $[\text{Ag}_2\text{NO}_3]^+$, Ag_3^+ , and $[\text{Ag}_3(\text{NO}_3)_2]^+$. The insets show the doublet and quadruplet patterns characteristic of Ag^+ and Ag_3^+ . The positive charge on Ag_3^+ might be intrinsic to the trimeric cluster, or it might be caused by oxidation during the electrospray ionization process. Therefore, the trimeric clusters of silver in aqueous AgNO_3 can be either positively charged (Ag_3^+) or neutral (Ag_3). The negative-mode mass spectrum (Figure S1 in the Supporting Information) indicates that there are also a number of negatively charged complexes in the aqueous AgNO_3 solution, with notable examples including $[\text{Ag}(\text{NO}_3)_2]^-$, $[\text{Ag}_2(\text{NO}_3)_3]^-$, and $[\text{Ag}_3(\text{NO}_3)_4]^-$. As established in previous work,

[*] Dr. Y. Xiong, I. Washio, Dr. J. Chen, Dr. M. Sadilek, Prof. Y. Xia
Department of Chemistry
University of Washington
Seattle, WA 98195 (USA)
Fax: (+1) 206-685-8665
E-mail: xia@chem.washington.edu

[**] This work was supported by the NSF (DMR-0451788). Y.X. is a Camille Dreyfus Teacher Scholar (2002–2007). I.W. is a visiting student from Tokyo Institute of Technology partially supported by a fellowship from the Japan Society for the Promotion of Science (JSPS) for young scientists. This work used the Nanotech User Facility (NTUF) at the UW, a member of the National Nanotechnology Infrastructure Network (NNIN) funded by the NSF.

Supporting information for this article is available on the WWW under <http://www.angewandte.org> or from the author.

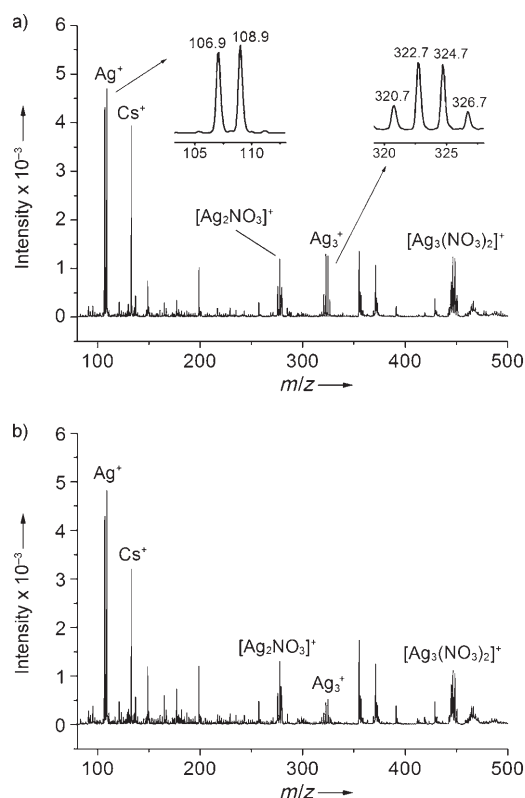


Figure 1. Positive-mode mass spectra of a 1 mM AgNO_3 aqueous solution: a) freshly prepared and b) after aging in air for 24 h. The insets in (a) clearly show the characteristic patterns for Ag^+ and Ag_3^+ . For both experiments, 0.1 mM CsNO_3 was added to the solution as a reference to calibrate the concentrations of silver species.

the $[\text{Ag}_2\text{NO}_3]^+$, $[\text{Ag}_3(\text{NO}_3)_2]^+$, $[\text{Ag}(\text{NO}_3)_2]^-$, $[\text{Ag}_2(\text{NO}_3)_3]^-$, and $[\text{Ag}_3(\text{NO}_3)_4]^-$ ions are complexes formed by Ag^+ ions with bridging nitrate groups.^[12] Thus, these complexes do not contain zero-valent silver atoms and should not be considered as nuclei for the formation of silver nanocrystals. To quantify the concentrations of silver species in solution, 0.1 mM CsNO_3 was added to the solution as a reference. Cesium has only one naturally occurring stable isotope, with an atomic mass of 133 amu. Thus, Cs^+ ions simply appear as a singlet at m/z 133 in the mass spectrum (Figure 1). Since Cs^+ ions are stable in aqueous medium for a long period of time, they can serve as a good reference for calibrating the concentrations of silver species obtained from the mass spectra of different samples. Note that the peaks in the regions 150–200 amu and 350–400 amu came from contamination by the tips of plastic micropipettes used to prepare samples for mass spectrometry (see Figure S2 in the Supporting Information). When we prepared the AgNO_3 stock solutions for nanoplate synthesis, the plastic micropipettes were replaced with glass pipettes to avoid contamination.

Further studies revealed that the concentration of trimeric clusters of silver decreased as the AgNO_3 solution was aged in air under ambient conditions (Figure S3 in the Supporting Information). Figure 1b shows a mass spectrum of the same AgNO_3 solution as in Figure 1a after it had been stored in a glass vial wrapped with aluminum foil for 24 h. The intensity

of the Ag_3^+ peak decreased, while the peaks of other ionic species increased. By calibrating against the added Cs^+ ions, we obtained the concentrations of all positively charged silver species at different times, which are plotted in Figure 2. In the freshly prepared solution, about 27% of the total silver is found in trimeric clusters. After the solution had been aged

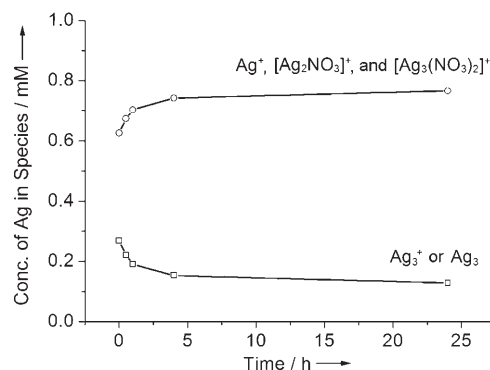


Figure 2. Plots showing the dependence of the concentrations of different silver species (given as concentration of silver atoms and ions) versus time, when a 1 mM aqueous AgNO_3 solution was aged in air. The lower trace (\square) shows the concentration of trimeric clusters of silver, and the upper trace (\circ) represents the total concentration of Ag^+ , $[\text{Ag}_2(\text{NO}_3)]^+$, and $[\text{Ag}_3(\text{NO}_3)_2]^+$. The concentration of each species was determined by integrating the peak areas in the mass spectra shown in Figures 1 and S2 (in the Supporting Information), with the Cs^+ signal as a reference.

for 24 h, only 13% of the silver still remained in the trimeric clusters. The number of silver atoms coming from the diminished trimeric clusters was essentially equal to the number of newly formed Ag^+ ions (including their complexes with NO_3^- ions). This conservation of silver implies that the trimeric clusters of silver were mainly transformed into Ag^+ ions and their nitrate complexes during the course of aging. It is still not clear how exactly this transformation occurs. We suspect the involvement of oxygen, a component that should be present in the aqueous medium or later dissolved from the air. Therefore, the most important parameter for controlling the concentration of trimetric clusters is the period of time during which the AgNO_3 solution is exposed to air. It is worth noting that the Ag^+ ions (and their complexes with NO_3^- ions) all in the +1 oxidation state, which is higher than the zero-valent silver in either Ag_3^+ or Ag_3 .

Photoinduced luminescence also provides evidence to support the existence of silver clusters. As shown in previous studies, silver clusters may exhibit photoluminescence signatures under appropriate conditions. For example, neutral Ag_n ($n = 2$ –10) clusters in rare-gas matrixes could emit light at a cryogenic temperature.^[13] Some investigations on silver particles in glass after treatment at 100 °C suggested that small silver clusters such as Ag_2^+ and Ag_3^{2+} could show broad-band photoluminescence centered at 600 nm with excitation at 400 nm.^[14] A recent study showed that Ag_{4+x}^{x+} clusters in solution emitted light around 550 nm when excited with a light source at 350 nm.^[15] We recorded a photoluminescence spectrum (Figure S4 in the Supporting Information) directly

from the commercial AgNO_3 powder excited at 275 nm and found a number of well-defined peaks in the range of 420–530 nm. Figure S4 in the Supporting Information also shows a photoluminescence spectrum recorded from freshly prepared aqueous AgNO_3 solution, which displays a broad band of emission centered at 475 nm. The spectrum resembles that of AgNO_3 powder except for its weaker intensity. When the aqueous solution was aged under ambient conditions, the photoluminescence gradually decreased until it became undetectable (Figure S4 in the Supporting Information). Since mass spectrometry has shown that the number of trimeric clusters was reduced with increasing aging time, these photoluminescence peaks might be associated with the trimeric clusters of silver.^[16] In this case, the trimeric clusters should originally be present in commercial AgNO_3 powder. We also noticed that the number of trimeric clusters only dropped when the AgNO_3 was dissolved in water and then aged in air. When the AgNO_3 was kept as a solid and exposed to room light for more than one month, the number of trimeric clusters, as revealed by mass spectrometry, did not change.

The positively charged Ag_3^+ cluster is a trimer whose ground state has an equilateral-triangular structure ($^1\text{A}_1$) and D_{3h} symmetry.^[17] The linear $^1\Sigma_g$ state is predicted to lie approximately 1 eV above the $^1\text{A}_1$ state. Thus, the Ag_3^+ cluster should exist as a triangle, in the lowest-energy state. Similarly, the ground state of the neutral Ag_3 cluster is a $^2\text{E}'$ state with an equilateral-triangular structure (D_{3h} symmetry).^[17] We suspect that, in a solution-phase synthesis, the trimeric clusters of silver can serve as nucleation sites onto which the newly formed silver atoms will be added to generate larger seeds and then nanocrystals. The triangular configuration of the trimeric clusters may naturally result in a triangular shape for the nuclei and thus for the final products. We tried to validate this hypothesis by performing a set of syntheses with aqueous solutions of AgNO_3 that contained the same amount of AgNO_3 but had been aged in air for different periods of time. As described above, the number of trimeric clusters in the AgNO_3 solution is reduced during the aging process. If the trimeric clusters indeed act as nuclei for newly formed silver atoms, the final products—triangular nanoplates of silver—would have larger lateral dimensions, since the number of trimeric clusters was reduced. We chose to use the hydroxyl end groups of poly(vinyl pyrrolidone) (PVP) to reduce AgNO_3 , because neither citrate nor light was found to be a prerequisite for forming triangular nanoplates through this route.^[8] Figure 3 shows SEM images of four samples that were prepared from aqueous AgNO_3 solutions that had been aged for 0, 1, 4, and 24 h (Figures 3a–d, respectively) before the reductant (PVP) was introduced. When the freshly prepared AgNO_3 solution was used, the product consisted of silver triangular nanoplates with an average edge length of about 300 nm. When the solution was aged for 1 h, the edge length increased to 350 nm. As the aging time was prolonged to 4 and 24 h, the edge length of products was further increased to 430 nm and 500 nm, respectively. This dependence of nanoplate edge length on the number of trimeric clusters implies that the trimeric clusters serve as nucleation sites. At the same concentration of AgNO_3 precursor, a decrease in the number

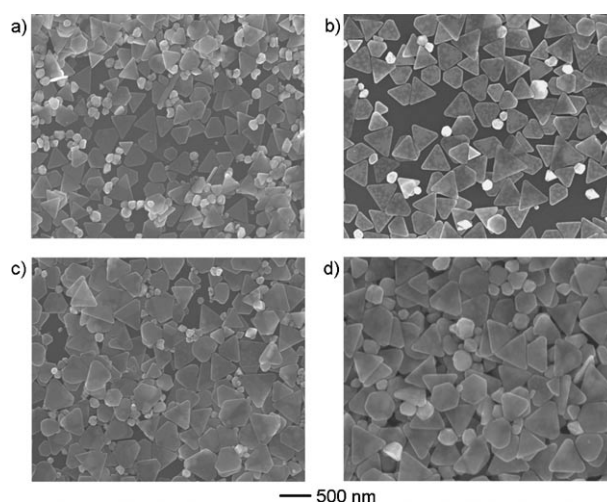


Figure 3. SEM images of samples prepared with an aqueous stock solution of AgNO_3 that had been aged for different periods of time: a) 0 h, b) 1 h, c) 4 h, and d) 24 h. As the aging of stock solutions was prolonged, the edge length of the final products increased.

of nuclei results in the production of nanoparticles with larger sizes.^[18]

The triangular nanoplates of silver only account for 80 % of the final products, with the other 20 % being cuboctahedrons and icosahedrons. We believe that these by-products were formed from the reduction of Ag^+ ions (as well as their complexes with NO_3^- ions) into silver atoms and subsequent homogeneous nucleation and growth. Figure 4 shows a comparison between the two nucleation mechanisms involved in a typical synthesis. In the first mechanism, the trimeric clusters serve as nucleation sites for the addition of newly

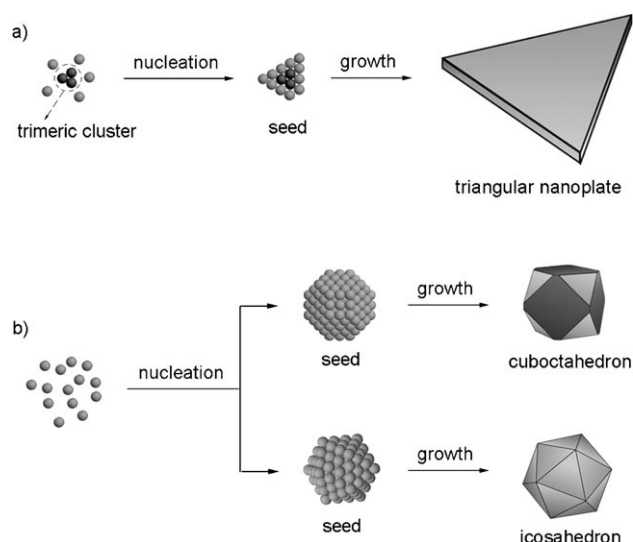


Figure 4. Schematic illustration of the formation of silver triangular nanoplates and nanocrystals of other shapes. a) The triangular nanoplates are formed with trimeric clusters serving as the nuclei. b) Icosahedrons and cuboctahedrons are formed owing to the self-nucleation of silver atoms. The Ag atoms are generated by reducing either Ag^+ or complexes such as $[\text{Ag}_2(\text{NO}_3)]^+$ and $[\text{Ag}_3(\text{NO}_3)_2]^+$ with PVP.

formed silver atoms. In this case, the silver atoms are generated by reducing Ag^+ ions (and their complexes with NO_3^- ions) with the hydroxyl end groups of PVP. Nucleation on the trimeric clusters produces triangular nuclei, which further evolve into platelike products as more silver atoms are added. During growth, the plates may either keep the triangular shape or be truncated, which depends on the ratio of {111} to {100} facets on the side faces.^[7] The hexagonal nanoplate, whose side faces are a mix of three {111} planes and three {100} planes, is an uttermost limit of this truncation. This argument is consistent with previous studies in which the shape of the final products was found to be largely determined by the morphology of nuclei.^[19] In the reaction system studied herein, a small portion of the newly formed silver atoms can self-nucleate into nuclei with different forms. These nuclei would then grow into cuboctahedrons and icosahedrons, as these two shapes are thermodynamically favorable.^[19,20] When the generation of Ag atoms is kept slow, the concentration of Ag atoms in the solution should be relatively low,^[18a,21] and thus the number of nuclei formed by self-nucleation would be limited. As a result, most of the Ag atoms tend to nucleate and grow on the trimeric clusters, so that triangular nanoplates of silver are obtained in a yield as high as 80%. In this synthesis, slow generation of Ag atoms (i.e. under kinetic control) is a prerequisite for the formation of triangular nanoplates of silver with high yields. If PVP is replaced with a stronger reductant, the reduction rate could become too fast, which would then ruin the shape control provided by the trimeric nuclei. Note that the complex ions, such as $[\text{Ag}_3(\text{NO}_3)_2]^+$ and $[\text{Ag}_3(\text{NO}_3)_4]^-$, cannot serve as nucleation sites as they do not contain zero-valent silver atoms and the silver cations in these complexes are separated by nitrate anions.^[12]

This work demonstrates the intrinsic driving force responsible for forming platelike nanostructures of silver in an isotropic medium. However, it is worth emphasizing that the morphology of a nanocrystal is determined by the interplay of many parameters. For example, as we have observed in previous studies, citrate ions can preferentially interact with {111} facets of silver nanocrystals.^[6c] Since triangular nanoplates of silver are bound by two {111} planes as the top and bottom faces and three {100} planes as the side faces,^[22] the preferential adsorption of citrate on {111} facets can help maintain the platelike morphology of silver nanocrystals during the growth process.^[6c] Furthermore, a slow addition rate for the newly formed atoms is also crucial to the formation of platelike morphology. If atomic addition is too fast, the trimeric clusters of silver may evolve into structures other than triangular nanoplates. In other words, the triangular trimeric clusters can only induce a platelike morphology in the nucleation stage. It is, however, clear that any successful synthesis of triangular nanoplates needs a careful control over both the nucleation and growth steps.

In summary, we have identified trimeric clusters of silver as an abundant species in commercial AgNO_3 powders and their aqueous solutions. We have also demonstrated the potential role of such clusters as nucleation sites in the formation of triangular nanoplates of silver. This work explains, for the first time, why slow generation of silver

atoms in a solution phase (i.e. in a kinetically controlled process) can lead to the formation of platelike nanostructures. This work presents a simple method based on the manipulation of nuclei concentration for controlling and tuning the lateral dimensions of silver nanoplates. Furthermore, this work paves the way in addressing a long-standing problem in chemistry and physics—understanding and control of nucleation involved in the formation of nanocrystals. There is no doubt that a better understanding of the nucleation step holds the key to better control over the shape and size of nanocrystals.^[23]

Experimental Section

In a typical synthesis,^[8] a 20-mL vial (liquid scintillation vial with a white cap and polyethylene liner, Research Products International, Chicago, IL) was wrapped with aluminum foil to block light. The vial was filled with water (5.0 mL) and silver nitrate (0.160 g; Aldrich, No. 209139-100G) and then capped. The solution was stored at room temperature for different periods of time up to 24 h. At the same time, poly(vinyl pyrrolidone) (PVP, 1.878 g; Aldrich, $M_w = 29000$) was dissolved in water (8.0 mL) in another 20-mL vial and heated to 60°C in air with magnetic stirring. After the aqueous AgNO_3 solution had been added (3.0 mL; the molar ratio between the repeating unit of PVP and AgNO_3 was 30), the vial was immediately capped, and heating was continued at 60°C for 21 h. The final product was collected by centrifugation and washed with water three times to remove excess PVP. The water involved in all syntheses was obtained by filtering through millipore cartridges (E-pure, Dubuque, IA). The samples were then characterized by scanning electron microscopy (SEM). SEM images were taken on an FEI field-emission scanning electron microscope (Sirion XL) that was operated at an accelerating voltage of 15 kV. Samples for SEM studies were prepared by placing a drop of the aqueous suspension of Ag nanoplates on a piece of silicon wafer under ambient conditions; the sample was then dried and stored in vacuum for SEM characterization.

Mass spectra were taken from aqueous solutions of AgNO_3 using a Bruker Esquire LC-ion trap mass spectrometer with an electrospray ion source operating in a positive or negative mode. For sample preparation, AgNO_3 (0.017 g) and water (10 mL) were added to a 20-mL vial to make a 10 mM aqueous solution, which was then diluted to 1 mM in a 20-mL vial wrapped with aluminum foil. CsNO_3 was also added at a concentration of 0.1 mM to serve as a reference to calibrate the concentrations of Ag species. The solution containing both AgNO_3 and CsNO_3 was aged in air for different periods of time up to 24 h, and an aliquot of 0.2 mL was removed at each point for mass spectrometry. The accumulation time for all the mass spectra was set to 1 min. The photoluminescence spectra of AgNO_3 powders and aqueous solutions were recorded on a Perkin Elmer LS-50B luminescence spectrophotometer with an excitation light source at 275 nm.

Received: March 2, 2007

Published online: May 24, 2007

Keywords: cluster compounds · crystal growth · nanostructures · silver · template synthesis

- [1] a) S. Nie, S. R. Emory, *Science* **1997**, 275, 1102; b) O. D. Velev, E. W. Kaler, *Langmuir* **1999**, 15, 3693; c) S. R. Nicewarner-Peña, R. G. Freeman, B. D. Reiss, L. He, D. J. Peña, I. D. Walton, R. Cromer, C. D. Keating, M. J. Natan, *Science* **2001**, 294, 137; d) Y. C. Cao, R. Jin, C. A. Mirkin, *Science* **2002**, 297, 1536;

- e) L. A. Dick, A. D. McFarland, C. L. Haynes, R. P. Van Duyne, *J. Phys. Chem. B* **2002**, *106*, 853; f) A. P. Alivisatos, *Nat. Biotechnol.* **2004**, *22*, 47.
- [2] a) U. Kreibitz, M. Vollmer, *Optical Properties of Metal Clusters*, Springer, New York, **1995**; b) T. R. Jensen, L. Kelly, A. Lazarides, G. C. Schatz, *J. Cluster Sci.* **1999**, *10*, 295; c) J. P. Kottmann, O. J. F. Martin, D. R. Smith, S. Schultz, *Phys. Rev. B* **2001**, *64*, 235402; d) M. Muniz-Miranda, *Chem. Phys. Lett.* **2001**, *340*, 437; e) I. O. Sosa, C. Noguez, R. G. Barrera, *J. Phys. Chem. B* **2003**, *107*, 6269; f) B. J. Wiley, S. H. Im, Z.-Y. Li, J. M. McLellan, A. Siekkinen, Y. Xia, *J. Phys. Chem. B* **2006**, *110*, 15666; g) F. Li, Z. Wang, A. Stein, *Angew. Chem.* **2007**, *119*, 1917; *Angew. Chem. Int. Ed.* **2007**, *46*, 1885.
- [3] a) K. L. Kelly, E. Coronado, L. L. Zhao, G. C. Schatz, *J. Phys. Chem. B* **2003**, *107*, 668; b) L. J. Sherry, R. Jin, C. A. Mirkin, G. C. Schatz, R. P. Van Duyne, *Nano Lett.* **2006**, *6*, 2060.
- [4] a) M. Duval Malinsky, K. L. Kelly, G. C. Schatz, R. P. Van Duyne, *J. Phys. Chem. B* **2001**, *105*, 2343; b) M. D. Malinsky, K. L. Kelly, G. C. Schatz, R. P. Van Duyne, *J. Am. Chem. Soc.* **2001**, *123*, 1471.
- [5] a) R. Jin, Y. Cao, C. A. Mirkin, K. L. Kelly, G. C. Schatz, J. G. Zheng, *Science* **2001**, *294*, 1901; b) Y. Sun, B. Mayers, Y. Xia, *Nano Lett.* **2003**, *3*, 675.
- [6] a) S. Chen, D. L. Carroll, *Nano Lett.* **2002**, *2*, 1003; b) S. Chen, Z. Fan, D. L. Carroll, *J. Phys. Chem. B* **2002**, *106*, 10777; c) I. Pastoriza-Santos, L. M. Liz-Marzán, *Nano Lett.* **2002**, *2*, 903; d) M. Maillard, S. Giorgio, M.-P. Pileni, *Adv. Mater.* **2002**, *14*, 1084; e) Y. Sun, Y. Xia, *Adv. Mater.* **2003**, *15*, 695; f) G. S. Métraux, C. A. Mirkin, *Adv. Mater.* **2005**, *17*, 412.
- [7] a) A. I. Kirkland, D. A. Jefferson, D. G. Duff, P. P. Edwards, I. Gameson, B. F. G. Johnson, D. J. Smith, *Proc. R. Soc. London Ser. A* **1993**, *440*, 589; b) Y. Xiong, J. M. McLellan, J. Chen, Y. Yin, Z.-Y. Li, Y. Xia, *J. Am. Chem. Soc.* **2005**, *127*, 17118.
- [8] a) I. Washio, Y. Xiong, Y. Yin, Y. Xia, *Adv. Mater.* **2006**, *18*, 1745; b) Y. Xiong, I. Washio, J. Chen, H. Cai, Z.-Y. Li, Y. Xia, *Langmuir* **2006**, *22*, 8563.
- [9] M. D. Hollingsworth, *Science* **2002**, *295*, 2419.
- [10] A. Henglein, *Chem. Phys. Lett.* **1989**, *154*, 473.
- [11] J. Belloni, M. Mostafavi, H. Remita, J. L. Marignier, M. O. Delcourt, *New J. Chem.* **1998**, *22*, 1239.
- [12] B. Antonioli, J. K. Clegg, D. J. Bray, K. Gloe, K. Gloe, H. Heßke, L. F. Lindoy, *CrystEngComm* **2006**, *8*, 748.
- [13] a) L. König, I. Rabin, W. Schultze, G. Ertl, *Science* **1996**, *274*, 1353; b) C. Félix, C. Sieber, W. Harbich, J. Buttet, I. Rabin, W. Schultze, G. Ertl, *Phys. Rev. Lett.* **2001**, *86*, 2992.
- [14] a) Y. Watanabe, G. Namikawa, T. Onuki, K. Nishio, T. Tsuchiya, *Appl. Phys. Lett.* **2001**, *78*, 2125; b) I. Belharouak, F. Weill, C. Parent, G. Le Flem, B. Moine, *J. Non-Cryst. Solids* **2001**, *293–295*, 649; c) A. V. Podlipensky, V. Grebenev, G. Seifert, H. Graener, *J. Lumin.* **2004**, *109*, 135.
- [15] M. Treguer, F. Rocco, G. Lelong, A. L. Nestour, T. Cardinal, A. Maali, B. Lounis, *Solid State Sci.* **2005**, *7*, 812.
- [16] W. Schulze, I. Rabin, G. Ertl, *ChemPhysChem* **2004**, *5*, 403.
- [17] a) J. Flad, G. Igel-Mann, H. Preuss, H. Stoll, *Chem. Phys.* **1984**, *90*, 257; b) P. Y. Cheng, M. A. Duncan, *Chem. Phys. Lett.* **1988**, *152*, 341; c) K. Balasubramanian, P. Y. Feng, *Chem. Phys. Lett.* **1989**, *159*, 452; d) H. Partridge, C. W. Bauschlicher, Jr., S. R. Langhoff, *Chem. Phys. Lett.* **1990**, *175*, 531; e) D. W. Boo, Y. Ozaki, L. H. Andersen, W. C. Lineberger, *J. Phys. Chem. A* **1997**, *101*, 6688; f) M. Hartmann, A. Heidenreich, J. Pittner, V. Bonačić-Koutecký, J. Jortner, *J. Phys. Chem. A* **1998**, *102*, 4069.
- [18] a) I. V. Markov, *Crystal Growth for Beginners*, World Scientific Publisher, Singapore, **1995**; b) Y. Xiong, J. Chen, B. Wiley, Y. Xia, Y. Yin, Z.-Y. Li, *Nano Lett.* **2005**, *5*, 1237.
- [19] a) C. Lofton, W. Sigmund, *Adv. Funct. Mater.* **2005**, *15*, 1197; b) B. Wiley, Y. Sun, J. Chen, H. Cang, Z.-Y. Li, X. Li, Y. Xia, *MRS Bull.* **2005**, *30*, 356; c) J. L. Elechiguerra, J. Reyes-Gasga, M. J. Yacaman, *J. Mater. Chem.* **2006**, *16*, 3906.
- [20] a) G. Wulff, *Z. Kristallogr.* **1901**, *34*, 449; b) L. D. Marks, *Rep. Prog. Phys.* **1994**, *57*, 603; c) A. Pimpinelli, J. Villain, *Physics of Crystal Growth*, Cambridge University Press, Cambridge, UK, **1998**.
- [21] a) T. Nomura, M. Alonso, Y. Kousaka, K. Tanaka, *J. Colloid Interface Sci.* **1998**, *203*, 170; b) T. Nomura, Y. Kousaka, M. Alonso, M. Fukunaga, T. Satoh, *J. Colloid Interface Sci.* **2000**, *221*, 195; c) R. P. Sear, *J. Phys. Chem. B* **2006**, *110*, 4985.
- [22] V. Germain, J. Li, D. Ingert, Z. L. Wang, M. P. Pileni, *J. Phys. Chem. B* **2003**, *107*, 8717.
- [23] a) J. Li, X. Li, H.-J. Zhai, L.-S. Wang, *Science* **2003**, *299*, 864; b) H.-F. Zhang, M. Stender, R. Zhang, C. Wang, J. Li, L.-S. Wang, *J. Phys. Chem. B* **2004**, *108*, 12259.